

Complexity from the Reduced Density Matrix: a *new* Diagnostic for Chaos

Arpan Bhattacharyya^{a1}, S. Shajidul Haque^{b2} and Eugene H. Kim^{c3}

^a*Indian Institute of Technology, Gandhinagar, Gujarat-382355, India*

^b *High Energy Physics, Cosmology & Astrophysics Theory Group
and The Laboratory for Quantum Gravity & Strings,
Department of Mathematics and Applied Mathematics,
University of Cape Town, South Africa*

^c*Department of Physics, University of Windsor,
Windsor, Ontario N9B 3P4 Canada*

ABSTRACT

We investigate circuit complexity to characterize chaos in multiparticle quantum systems; concomitantly, we take strides in using complexity to characterize open quantum systems. By exploring different types of quantum circuits, we propose a new diagnostic of chaos from complexity based on the reduced density matrix. Through explicit calculations on a model of two coupled harmonic oscillators where one or both of the oscillators are inverted, we demonstrate that the evolution of complexity is an effective diagnostic of chaos.

¹abhattacharyya@iitgn.ac.in

²shajid.haque@uct.ac.za

³ehkim@uwindsor.ca

Contents

1	Introduction	1
2	Our Model and Complexity	3
3	System Complexity	6
4	Complexity from the Reduced Density Matrix	11
4.1	Complexity from Operator State Mapping	11
4.2	Complexity of Purification	17
5	Discussion	19

1 Introduction

Chaotic systems are abundant in nature. Although we have a reasonably thorough understanding of classical chaos, our knowledge of chaos for quantum systems is still inadequate [1, 2]. We expect quantum chaos to play an essential role in our understanding of some of the most important open questions in physics such as thermalization, transport in quantum many-body systems, black hole information loss etc. Therefore, it is essential to have a comprehensive understanding of quantum chaos [1, 2].

Traditionally, chaos in quantum systems has been identified by comparison with results from random matrix theory (RMT) [2, 3]. Recently, however, other diagnostics have been proposed to probe chaotic quantum systems. One such diagnostic is the out-of-time-ordered correlator (OTOC), $F_T(t) \equiv \langle W(t)V(0)W(t)V(0) \rangle$, where $W(t)$ and $V(t)$ are operators in the Heisenberg picture, and the angle bracket $\langle \cdots \rangle$ denotes a thermal average. This quantity has been argued to give information about the chaos in quantum mechanical systems [4–6]. It has been shown that the (classical) Lyapunov exponent and the scrambling time may be extracted from these quantities. However, recent works have revealed some tension between the OTOC and RMT diagnostics [7]. A deeper understanding of probes of quantum chaos is required; it is worthwhile to investigate other probes of quantum chaos. Quantum

information theory turns out to be the most promising in this direction.

Ideas and tools from quantum information theory have come to permeate all of modern (quantum) physics. They have brought new insights into traditional ideas and had far-reaching consequences, e.g. a new perspective in the structure of space-time itself. Most information-theoretic studies begin by (purposely) partitioning the system into subsystems A and B ; one considers the reduced density matrix of subsystem- A , upon tracing out subsystem- B , $\hat{\rho}_A = \text{Tr}_B[\hat{\rho}]$, where $\hat{\rho}$ is the density matrix of the entire system and the *von Neumann entropy*, $S = -\text{Tr}[\hat{\rho}_A \ln \hat{\rho}_A]$. Indeed, much of quantum information theory is concerned with the uses and interpretation of the von Neumann entropy.

An information-theoretic quantity which has recently come into the limelight is the system's *complexity*. Complexity, rather ‘Circuit Complexity’ [8–10], is an idea from the theory of quantum computation — it is the shortest distance between some reference states $|\psi_R\rangle$ and a target state $|\psi_T\rangle$. Operationally, it quantifies the minimal number of operations needed to manipulate $|\psi_R\rangle$ to $|\psi_T\rangle$. The flurry of recent work on circuit complexity in the field of quantum field theory in recent time [11–37] has largely been spurred by black hole physics and, in particular, the conjecture that it resolves certain puzzles related to black holes [38, 39]. The aspect of complexity that we are particularly interested in is its potential to characterize quantum chaos. Previous work [40–46] has shown that complexity could detect the scrambling time and Lyapunov exponent. However, this required a unique type of quantum circuit — a doubly-evolved state, where the target state is obtained by first evolving the system forward in time with a Hamiltonian H , and then evolving it backwards in time with a slightly different Hamiltonian $H + \delta H$.

In this work, we take the first step toward using complexity to characterize chaos in a multiparticle system. We consider two coupled oscillators, where one or both of the oscillators are inverted. It is well known that, classically, the inverted oscillator has an unstable fixed point in phase space at $(x = 0, p = 0)$ (and, hence, not chaotic in the strict sense). Nonetheless, in the context of studying quantum chaos in various quantum field theories [47–55], it has served as a powerful toy model mostly because it is an exactly solvable system. We begin by revisiting the complexity of the doubly-evolved circuit state, namely a state obtained by first evolving the system forward in time with a Hamiltonian H , and then evolving it backwards in time with a Hamiltonian $H + \delta H$. We highlight some new features that were not appreciated in previous works [40]. We discovered that in the inverted regime the complexity for this doubly evolved state and a single evolved state with respect to the

same reference state saturate at the same value. When the parameters for the system and bath are different, the linear growth region of complexity splits into two separate regions, indicating the Lyapunov spectrum [56].

Then we propose a new diagnostic of chaos using complexity that does not require this type of contrived target state and is, in fact, more powerful. This new diagnostic is based on the reduced density matrix by employing the “operator-state mapping” [57–59] to build an effective target state. Our proposal captures all the features mentioned above and more. For example, we found that the scrambling time and Lyapunov exponents are mainly dictated by the bath parameter. Finally, we also compare this new form of complexity with the complexity of purification [17, 28, 60–63] for detecting chaos. We discover that the complexity of purification is not as sensitive as our proposed probe.

It should be noted, the model we consider can be thought of as the simplest example of an *open quantum system*, where some subsystem is treated as the ‘system’, and the rest is treated as a ‘bath/reservoir’ [47]. Open quantum systems are extremely important for various reasons [64–66]. Our proposal takes a step toward using complexity to characterize open quantum systems. Previously in [25, 26], a system connected with a classical source was considered; however, the diagnostic used was the full system complexity.

The rest of the paper is organized as follows. In Section 2, we present our model and a brief review of circuit complexity. In Section 3, we compute the evolution of complexity for the entire system for different circuits and demonstrate how quantum chaos can be detected and quantified. In Section 4, we illustrate our new proposal as the diagnostic of chaos and compare it with the complexity of purification. Finally, we summarize and present concluding remarks in Section 5.

2 Our Model and Complexity

Our model consists of two oscillators, where we treat one of the oscillators as the system and the other as the environment. The Hamiltonian of our model is the following

$$H = \frac{1}{2}p_1^2 + \frac{\omega_0^2\epsilon_1}{2}x_1^2 + \frac{1}{2}p_2^2 + \frac{\omega_0^2\epsilon_2}{2}x_2^2 + \lambda\omega_0^2x_1x_2 . \quad (2.1)$$

Here x_i and p_i are the position and momentum operators at site- i , with $[x_i, p_j] = i\delta_{i,j}$, ω_0 is a parameter with units of energy and $\{\epsilon_1, \epsilon_2, \lambda\} \in \mathbf{R}$ are dimensionless parameters. In what follows, we take $\lambda \geq 0$; we set $\omega_0 = 1$, i.e. ω_0 sets the energy scale. We are working in units where $\hbar = 1$. The Hamiltonian (Eq. 2.1) is readily diagonalized by introducing a matrix notation —

$$\mathbf{x} = \begin{pmatrix} x_1 \\ x_2 \end{pmatrix}, \quad \mathbf{p} = \begin{pmatrix} p_1 \\ p_2 \end{pmatrix}, \quad \hat{K} = \begin{pmatrix} \epsilon_0 & \lambda \\ \lambda & -\epsilon_0 \end{pmatrix}, \quad (2.2a)$$

where $\epsilon_0 = (\epsilon_1 - \epsilon_2)/2$. Using this matrix notation, the Hamiltonian takes the form

$$H = \frac{1}{2}\mathbf{p}^T \mathbf{p} + \frac{\omega_0^2}{2} \left(\frac{1}{2}(\epsilon_1 + \epsilon_2) \mathbf{x}^T \mathbf{x} + \mathbf{x}^T \hat{K} \mathbf{x} \right). \quad (2.2b)$$

By performing an orthogonal transformation, we can diagonalize this Hamiltonian (2.2b). Under this transformation we define new position and momentum variables Q_i and P_i ($[Q_i, P_j] = i\delta_{i,j}$) as

$$\mathbf{x} = S\mathbf{Q}, \quad \mathbf{p} = S\mathbf{P}, \quad (2.3)$$

where

$$\mathbf{Q} = \begin{pmatrix} Q_s \\ Q_a \end{pmatrix}, \quad \mathbf{P} = \begin{pmatrix} P_s \\ P_a \end{pmatrix} \quad \text{and} \quad S = \begin{pmatrix} u & -v \\ v & u \end{pmatrix} \quad (2.4)$$

with

$$u = \sqrt{\frac{1}{2} \left(1 + \frac{\epsilon_0}{E} \right)}, \quad v = \sqrt{\frac{1}{2} \left(1 - \frac{\epsilon_0}{E} \right)}, \quad \text{and} \quad u^2 + v^2 = 1, \quad E = \sqrt{\epsilon_0^2 + \lambda^2}. \quad (2.5)$$

Then Eq. 2.2b takes the form

$$H = \frac{1}{2}\mathbf{P}^T \mathbf{P} + \frac{\omega_0^2}{2} \left(\frac{\epsilon_1 + \epsilon_2}{2} \mathbf{Q}^T \mathbf{Q} + \mathbf{Q}^T \Lambda \mathbf{Q} \right) \quad (2.6)$$

where

$$\Lambda = \begin{pmatrix} E & 0 \\ 0 & -E \end{pmatrix}.$$

We can write this explicitly as follows:

$$H = \frac{1}{2}P_s^2 + \frac{\Omega_s^2}{2}Q_s^2 + \frac{1}{2}P_a^2 + \frac{\Omega_a^2}{2}Q_a^2, \quad (2.7)$$

where

$$\Omega_s^2 = \omega_0^2 \left(\frac{\epsilon_1 + \epsilon_2}{2} + E \right) , \quad \Omega_a^2 = \omega_0^2 \left(\frac{\epsilon_1 + \epsilon_2}{2} - E \right) . \quad (2.8)$$

The states we will consider originate from a quench in the above model —

$$\begin{aligned} H &= H_< : \{ \epsilon_1 = 1 , \epsilon_2 = 1 , \lambda = 0 \} && \text{for } t < 0 \\ H &= H_> : \{ \epsilon_1 \neq 1 , \epsilon_2 \neq 1 , \lambda > 0 \} && \text{for } t > 0 , \end{aligned} \quad (2.9)$$

Now we will give a brief review of circuit complexity. We will directly use the wavefunction and compute the circuit complexity using Nielsen's method [8–10]. The details can be found in [11]. The problem/goal of complexity is the following: given a set of elementary gates and a reference state, what is the most efficient quantum circuit that starts at that reference state (at $s = 0$) and terminates at a target state ($s = 1$)

$$|\Psi_{s=1}\rangle = U(s=1)|\Psi_{s=0}\rangle, \quad (2.10)$$

where U is the unitary operator that takes the reference state to the target state. We construct it from a continuous sequence of parametrized path ordered exponential of the Hamiltonian operator

$$U(s) = \overleftarrow{\mathcal{P}} \exp[-i \int_0^s ds' H(s')] . \quad (2.11)$$

Here s parametrizes a path in the space of the unitaries and given a set of elementary gates M_I , the Hamiltonian can be written as

$$H(s) = Y(s)^I M_I . \quad (2.12)$$

The coefficients Y^I are the control functions that dictates which gate will act at a given value of the parameter. The control function is basically a tangent vector in the space of unitaries and satisfy the Schrodinger equation

$$\frac{dU(s)}{ds} = -i Y(s)^I M_I U(s) . \quad (2.13)$$

Then we define a cost functional $\mathcal{F}(U, \dot{U})$ as follows:

$$\mathcal{C}(U) = \int_0^1 \mathcal{F}(U, \dot{U}) ds . \quad (2.14)$$

Minimizing this cost functional gives us the optimal circuit. There are different choices for the cost functional [11]. In this paper we will consider

$$\mathcal{F}_2(U, Y) = \sqrt{\sum_I (Y^I)^2}. \quad (2.15)$$

In this work we will consider the ground state of $H_<$, $|\psi_0\rangle$ as our reference state $|\psi_R\rangle$ and we will consider different target states $|\psi_T\rangle$ that are evolved from this ground state. The target wave function will have the following form: $\psi_T(x_1, x_2) = \langle x_1, x_2 | \psi_T \rangle$ takes the form

$$\psi_T(x_1, x_2) = \mathcal{N}(t) \exp \left(-\frac{1}{2} [\Omega_1(t)x_1^2 + \Omega_2(t)x_2^2 - 2\kappa(t)x_1x_2] \right), \quad (2.16)$$

where $\Omega_1(t), \Omega_2(t) \in \mathbf{C}$ (with $\text{Re}[\Omega_1(t)], \text{Re}[\Omega_2(t)] > 0$) and $\kappa(t), \mathcal{N}(t) \in \mathbf{R}$. In all the cases, the complexity takes the form [11, 67] (due to the structure of the wave functions)

$$\mathcal{C} = \frac{1}{2} \sqrt{\sum_{\alpha=s,a} \left(\ln \left(\frac{|\Omega_\alpha|}{\omega_0} \right)^2 + \tan^{-1} \left(-\frac{\text{Im}(\Omega_\alpha)}{\text{Re}(\Omega_\alpha)} \right)^2 \right)}, \quad (2.17)$$

where the $\{\Omega_\alpha\}$ are the normal mode frequencies.

In this work, we start with first the full system complexity and study the unstable behaviour by using the technique [40]. Then we will propose a new diagnostic for studying chaos from the reduced density matrix.

3 System Complexity

In this section, we discuss the complexity of the (entire) system. we consider two types of target states and study the evolution of complexity for the same reference state. First we consider a target state obtained by evolving the system forward in time by the Hamiltonian $H_>$

$$|\psi(t)\rangle = \exp(-iH_>t)|\psi_0\rangle. \quad (3.1)$$

Working in the position representation, the evolved wavefunction can be written as

$$|\psi(t)\rangle = \exp(-iH_>t)|\psi_0\rangle \longrightarrow \psi(\mathbf{x}, t) = \int d\mathbf{x}' K(\mathbf{x}, t|\mathbf{x}', t=0) \psi_0(\mathbf{x}'), \quad (3.2a)$$

where the initial wave function $\psi_0(\mathbf{x})$ has the form

$$\psi_0(\mathbf{x}) = \left(\frac{\det(\hat{\Omega}_0)}{\pi^2} \right)^{1/4} \exp \left(-\frac{1}{2} \mathbf{x}^T \hat{\Omega}_0 \mathbf{x} \right) , \quad (3.2b)$$

and $K(\mathbf{x}, \mathbf{x}'|t)$ is the propagator

$$K(\mathbf{x}, \mathbf{x}'|t) = \langle \mathbf{x} | \exp(-iH_{>}t) | \mathbf{x}' \rangle . \quad (3.2c)$$

For the Hamiltonian given in Eq. 2.1, the propagator factorizes in normal mode coordinates and the propagator for each normal mode is

$$K(Q_\alpha, Q'_\alpha|t) = \left(\frac{g_\alpha}{i2\pi} \right)^{1/2} \exp \left(\frac{i}{2} [f_\alpha(Q_\alpha^2 + Q'^2_\alpha) - 2g_\alpha Q_\alpha Q'_\alpha] \right) \quad (3.3)$$

where $f_\alpha = \omega_\alpha \cot(\omega_\alpha t)$, and $g_\alpha = \omega_\alpha / \sin(\omega_\alpha t)$. To carry out the calculations, we return to the original coordinates via Eq. 2.3. The propagator can be written as

$$K(\mathbf{x}, \mathbf{x}'|t) = \prod_\alpha \left(\frac{g_\alpha}{i2\pi} \right)^{1/2} \exp \left(\frac{i}{2} [(\mathbf{x}^T \hat{F} \mathbf{x} + \mathbf{x}'^T \hat{F} \mathbf{x}') - \mathbf{x} \hat{G} \mathbf{x}' - \mathbf{x}' \hat{G} \mathbf{x}] \right) , \quad (3.4a)$$

where

$$\hat{F} = S \begin{pmatrix} f_S & 0 \\ 0 & f_A \end{pmatrix} S^T , \quad \hat{G} = S \begin{pmatrix} g_S & 0 \\ 0 & g_A \end{pmatrix} S^T . \quad (3.4b)$$

Carrying out the Gaussian integrals, one obtains

$$\psi(\mathbf{x}, t) = \left(\frac{\det(\text{Re}[\hat{\Omega}(t)])}{\pi^2} \right)^{1/4} \exp \left(-\frac{1}{2} \mathbf{x}^T \hat{\Omega}(t) \mathbf{x} \right) , \quad (3.5)$$

where

$$\hat{\Omega}(t) = \hat{G}(\hat{\Omega}_0 - i\hat{F})^{-1}\hat{G} - i\hat{F} . \quad (3.6)$$

To get the other target state we evolve the system forward in time with a Hamiltonian $H_{>}^F$, and then backward in time with a slightly different Hamiltonian $H_{>}^B$:

$$|\psi(t)\rangle = \exp(+iH_{>}^B t) \exp(-iH_{>}^F t) |\psi_0\rangle . \quad (3.7)$$

For the case we can write in the position representation:

$$|\psi(t_2)\rangle = \exp(-iH_2t_2) \exp(-iH_1t_1)|\psi_0\rangle \longrightarrow \psi(\mathbf{x}, t_2) = \int d\mathbf{x}' d\mathbf{x}'' K_2(\mathbf{x}, \mathbf{x}|t_2) K_1(\mathbf{x}', \mathbf{x}''|t_1) \psi_0(\mathbf{x}'') , \quad (3.8)$$

where we are ultimately interested in $t_1 \rightarrow t$ and $t_2 \rightarrow -t$. Using the parameterization for the propagator in Eq. 3.4a and carrying out the (Gaussian) integrals, one obtains Eq. 3.5 with

$$\hat{\Omega}(t) = \hat{G}_2 \hat{M}_2^{-1} \hat{G}_2 - i\hat{F}_2 \quad \text{with} \quad \hat{M}_2 = \hat{G}_1 (\hat{K} - i\hat{F}_1)^{-1} \hat{G}_1 - i(\hat{F}_1 + \hat{F}_2) . \quad (3.9)$$

Then the wavefunction can be written as the desired form 2.17:

$$\psi(x_1, x_2) = \left(\frac{\det(\text{Re}[\hat{\Omega}(t)])}{\pi^2} \right)^{1/4} \exp \left(-\frac{1}{2} [\Omega_1(t)x_1^2 + \Omega_2(t)x_2^2 - 2\kappa(t)x_1x_2] \right) , \quad (3.10)$$

where

$$\Omega_1(t) = \hat{\Omega}(t)_{11} , \quad \Omega_2(t) = \hat{\Omega}(t)_{22} , \quad \kappa(t) = -\hat{\Omega}(t)_{12} . \quad (3.11)$$

For a chaotic quantum system, even if the two Hamiltonians are arbitrarily close, i.e.

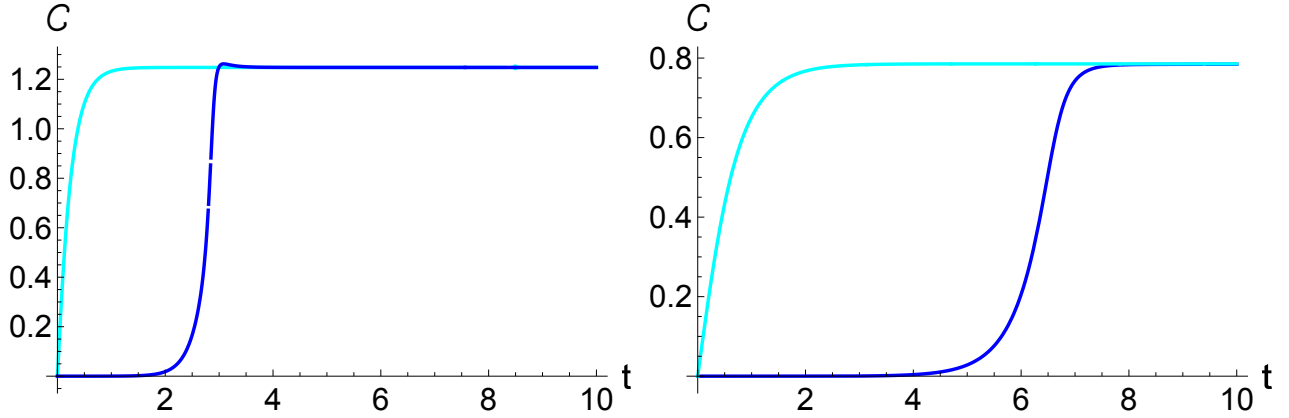


Figure 1: Left: Complexity for single evolved (in cyan) and doubly evolved (in blue) with $\epsilon_1 = -5, \epsilon_2 = -5, \lambda = 0.1, \delta\lambda = 0.001$ and **Right:** Complexity for single evolved (in cyan) and doubly evolved (in blue) with $\epsilon_1 = -1, \epsilon_2 = 1, \lambda = 0.1, \delta\lambda = 0.001$.

$H_{>}^B = H_{>}^F + \delta H_{>}^F$, the resulting state $|\psi_T\rangle$ will be quite different from $|\psi_0\rangle$. This type of evolved state is used to compute the Loschmidt echo [68–70], which is a measure of quantum chaos. It was pointed in [40] that the complexity for this type of doubly-evolved state 3.10 is essential to capture the chaotic behaviour of the system. The authors showed that complexity could capture similar information contained in the out-of-time order correlators

and, hence, can be used as an alternative diagnostic to study chaotic features. The time scale when complexity starts to grow linearly is equivalent to the scrambling time, and the slope of the linear portion captures the Lyapunov exponent.

In what follows, we employ this approach and consider the complexity associated with Eq. 3.7, comparing it with the complexity associated with Eq. 3.1; in doing so, we demonstrate a new feature of many-body unstable systems. We also demonstrate that the complexity associated with Eq. 3.7 is capable of sensing the system's Lyapunov spectrum. As highlighted above, since we are interested in chaotic behaviour, we focus on the case where either one of the oscillators or both are inverted ($\epsilon_1 < 0$, and/or $\epsilon_2 < 0$). Note that there are different ways to construct the perturbed Hamiltonian. For our simple model, we have three parameters: $\{\epsilon_1, \epsilon_2, \lambda\}$; we can construct the perturbed Hamiltonian $H + \delta H$ by considering perturbations of any combination of these parameters. Fig. 1 displays the evolution of com-

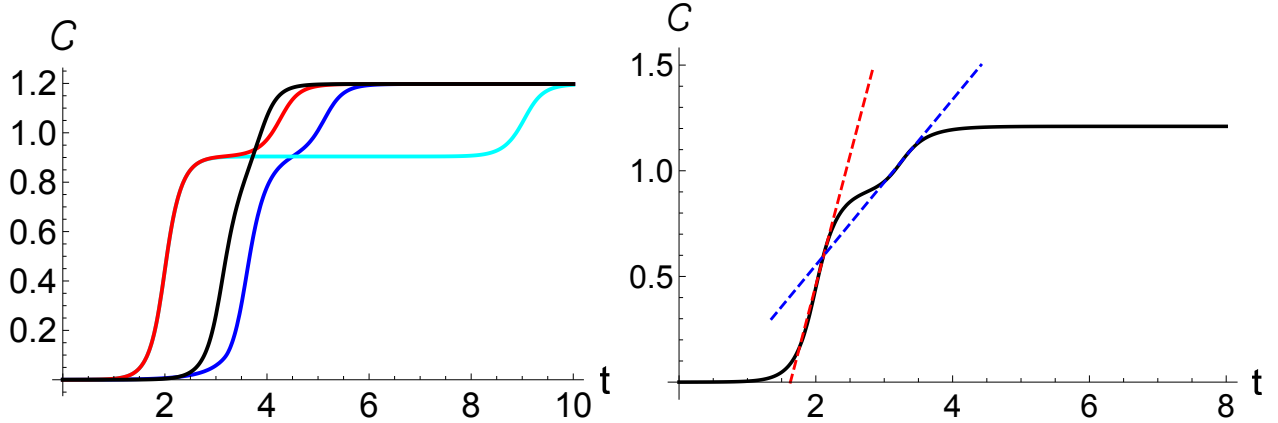


Figure 2: Left: Complexity for forward-backward evolved target state for perturbation in different directions with $\epsilon_1 = -6, \epsilon_2 = -1, \lambda = 0.1$ Cyan: $\delta\epsilon_1 = 0.001, \delta\epsilon_2 = 0, \delta\lambda = 0$, Blue: $\delta\epsilon_1 = 0, \delta\epsilon_2 = 0.001, \delta\lambda = 0$, Black: $\delta\epsilon_1 = 0, \delta\epsilon_2 = 0, \delta\lambda = 0.001$, Red: $\delta\epsilon_1 = 0.001, \delta\epsilon_2 = 0.001, \delta\lambda = 0$. **Right:** Complexity display different Lyapunov when ϵ parameters for the system and bath oscillators are different. Here we took $\epsilon_1 = -6, \epsilon_2 = -2, \lambda = 0.1, \delta\epsilon = 0.001, \delta\lambda = 0.001$ The two slopes are displayed by red and blue dashed lines.

plexity for the above mentioned target states, where $H + \delta H = H(\lambda + \delta\lambda)$. Notice that for both cases, the complexity is bounded. This behaviour was not seen in [40]; we believe this is due to the more sensitive nature of wave function method over the correlation matrix method. The complexity for the singly-evolved state (Eq. 3.1) grows rapidly and reaches saturation; the doubly-evolved state (Eq. 3.7) starts with a scrambling regime, grows linearly, and finally reaches its (maximum) saturation value. To our surprise, the complexity is bounded by the same values for both the singly-evolved and doubly-evolved states. We do not observe this

feature when either (or both) of the oscillators is (are) inverted. This is not surprising — for a regular system, the magnitude of the complexity increases when we evolve the system further. Therefore, this feature holds only when one or both oscillators of the system is/are unstable; hence one or both oscillators are inverted with fixed parameters. This implies a state obtained by evolving a state multiple times will have the same complexity after the scrambling time is over. Hence, it appears that, after a certain time scale, no target state is any more or less difficult to construct (from a particular reference state) than any other. This might have potential practical applications in information processing. Note that we

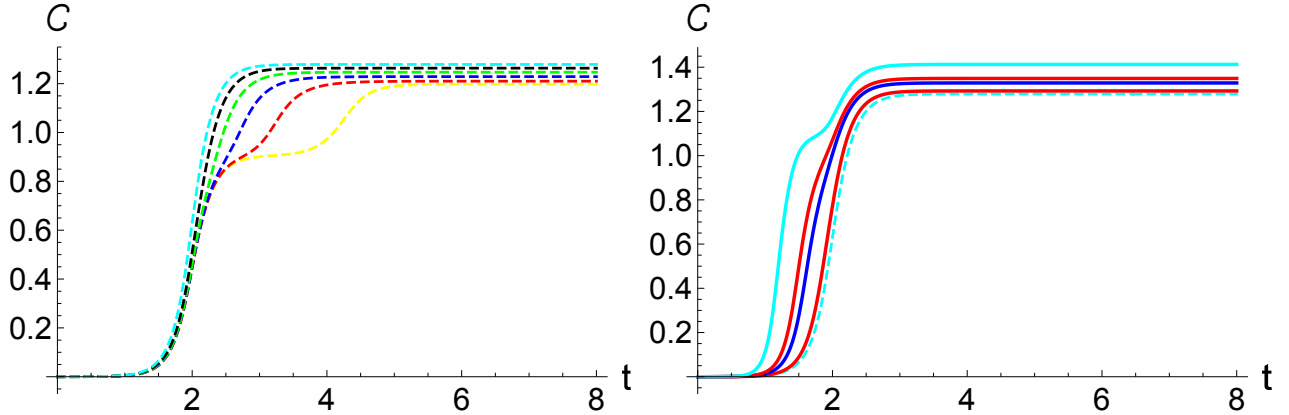


Figure 3: Complexity display two separate linear growths when the parameters (ϵ_1, ϵ_2) for the system and bath oscillators are different. In the left panel the bath parameter ϵ_2 is fixed at -6 and the system parameter ϵ_1 is scanning from -1 to -6. Whereas in the right panel, the system parameter ϵ_1 is chosen as -6, -7, -10, -12 and -20 from dashed cyan to solid cyan curve respectively.

can perform the backward evolution with the Hamiltonian, $H + \delta H = H(\epsilon_1 + \delta\epsilon_1, \epsilon_2 + \delta\epsilon_2, \lambda)$ i.e. we can perturb the Hamiltonian by slightly changing the parameters ϵ_1 and ϵ_2 . Fig. 2 displays how such a perturbation in different direction displays different complexity growth, though the qualitative feature of the growth is similar. The evolution of complexity for this type of perturbation demonstrates another interesting feature of our unstable system — when the parameters ϵ 's are quite different, the linear growth of complexity happens in two distinct segments with two different slopes. The right panel of Fig.2 shows that complexity is almost flat early time (scrambling), then it grows linearly; after that it flattens again (2nd scrambling) for a period, followed by a second linear growth and finally reaching saturation.

To make the connection more concrete, in Fig. 3 we fix either ϵ_1 or ϵ_2 and sweep through the other. Interestingly, the first linear growth and the first scrambling time is dictated by the fixed-parameter ϵ_2 . Fig. 3 displays the complexity for same $\epsilon_2 < 0$, for different choices

of $\epsilon_1 < 0$. As we increase $|\epsilon_2|$, the second scrambling time decreases and the slope of the second linear portion starts to align with the slope of the first linear portion as $\epsilon_1 \rightarrow \epsilon_2$. Finally, when the system parameter ($|\epsilon_1|$) is bigger than the bath parameter ($|\epsilon_2|$), the slope of the upper linear portion starts to bent in the opposite direction (see Fig. 3). We see the same behaviour when we fix the system parameter and scan through the bath parameter. This implies that complexity for this target state, cannot distinguish between the two. In the next section, we propose a new diagnostic that will be able to distinguish between the two. We conclude this section by commenting on the saturation value of the complexity when $H + \delta H = H(\epsilon_1 + \delta\epsilon_1, \epsilon_2 + \delta\epsilon_2, \lambda)$. If we increase the magnitude of either ϵ_1 and ϵ_2 or both the saturation value of complexity increases.

4 Complexity from the Reduced Density Matrix

In this section, we will propose a new diagnostic of chaos from complexity. First of all, this particular approach does not require the construction of the target state by performing two evolutions (forward followed by a backward with slightly different Hamiltonian) as discussed in the previous section. In that sense, this is a more natural diagnostic for studying chaotic behaviour. Secondly, it will capture all the features displayed in the previous section as well as some new ones. As noted above, our model can be thought of as the simplest open quantum system, where one of the oscillators is treated as the *system* and the other is treated as the *bath*. The reduced density matrix plus the operator-state mapping [57–59] form the basic ingredients for constructing the diagnostic. In the second part of this section, we will compare the results obtained from this approach with those obtained using the *complexity of purification*, showing that the complexity of purification captures less information.

4.1 Complexity from Operator State Mapping

We will be interested in analyzing the reduced density matrix. To that end, we partition the system into two subsystems, taking oscillator-1 to be our “system” and oscillator-2 to be the “bath”; we form the reduced density matrix of oscillator-1

$$\hat{\rho}_1 = \text{Tr}_2[\hat{\rho}] , \tag{4.1}$$

where $\hat{\rho}$ is the density matrix of the entire system. Calculations are readily executed in the

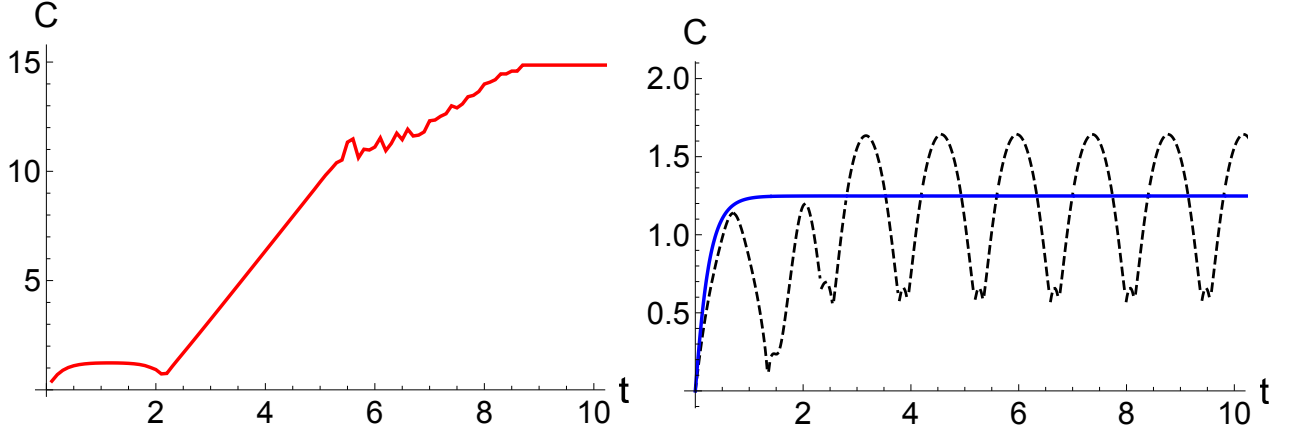


Figure 4: Complexity for the effective wave function when both oscillators are inverted (left panel) and when one of the oscillators are inverted. The parameters are – **Left:** $\epsilon_1 = -5.01, \epsilon_2 = -5, \lambda = 0.1$ and **Right:** black dashed curve has $\epsilon_1 = 5.01, \epsilon_2 = -5, \lambda = 0.1$ and the blue curve has $\epsilon_1 = -5.01, \epsilon_2 = 5, \lambda = 0.1$.

position representation —

$$\hat{\rho}_1 = \int dx_1 dx'_1 \rho_1(x_1, x'_1) |x_1\rangle \langle x'_1|, \quad (4.2a)$$

where

$$\rho_1(x_1, x'_1) = \int dq_2 \rho(x_1, q_2 | x'_1, q_2) \quad (4.2b)$$

with

$$\rho(x_1, x_2 | x'_1, x'_2) = \psi(x_1, x_2) \psi^*(x'_1, x'_2) \quad (4.2c)$$

being the position-space density matrix of the full system. The wave function is given by Eq. 3.10, namely

$$\psi(x_1, x_2) = \left(\frac{\text{Re}[\Omega_s(t)] \text{Re}[\Omega_a(t)]}{\pi^2} \right)^{1/4} \exp \left(-\frac{1}{2} [\Omega_1(t)x_1^2 + \Omega_2(t)x_2^2 - 2\kappa(t)x_1x_2] \right);$$

forming the system's position-space density matrix (Eq. 4.2c) and tracing out oscillator-2 (as per Eq. 4.2b), one obtains the reduced density matrix for oscillator-1

$$\rho_1(x_1, x'_1) = \sqrt{\frac{\gamma_1 - \eta}{\pi}} \exp \left(-\frac{1}{2} (\gamma x_1^2 + \gamma^* x_1'^2) + \eta x_1 x'_1 \right), \quad (4.3a)$$

where

$$\gamma = \Omega_1(t) - \kappa^2(t)/2\text{Re}[\Omega_2(t)] , \quad \eta = |\kappa(t)|^2/2\text{Re}[\Omega_2(t)] , \quad (4.3b)$$

and $\gamma_1 = \text{Re}[\gamma]$. In what follows, we will be particularly interested in powers of the reduced density matrix; we focus on $\hat{\rho}_1^{1/2}$ —

$$\rho_1^{1/2}(x, x') = \left(\frac{\gamma_1^2 - \eta^2}{\pi^2} \right)^{1/4} \exp \left(-\frac{1}{2}(\gamma + \eta)x^2 - \frac{1}{2}(\gamma^* + \eta)x'^2 + \sqrt{2\eta(\gamma_1 + \eta)}xx' \right) \quad (4.4)$$

Now we are ready to use the operator-state mapping [57–59]. The idea is for any operator,

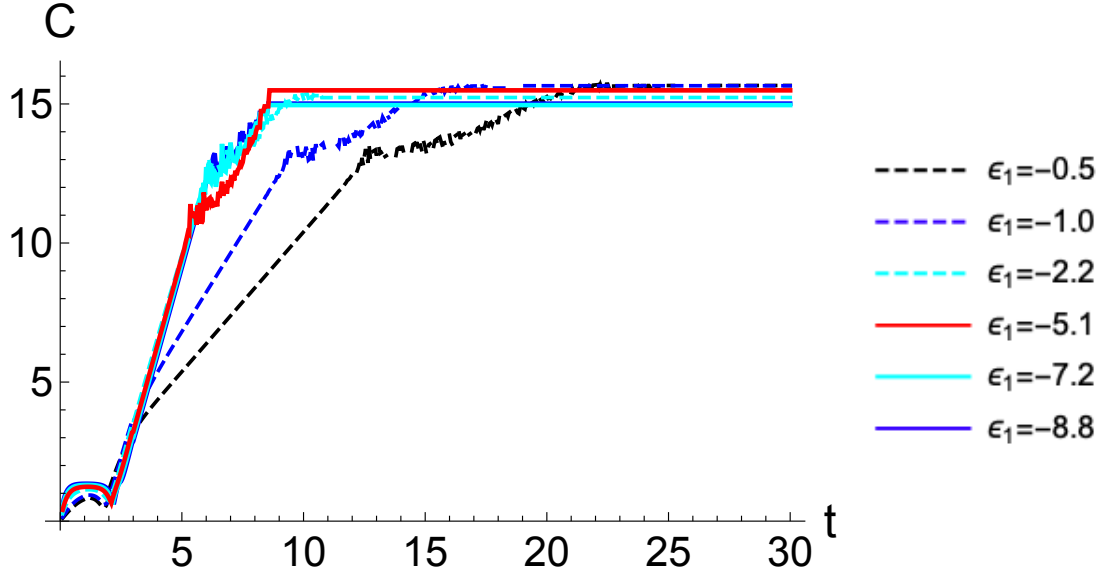


Figure 5: Complexity for $\epsilon_2 = -5, \lambda = 0.1$

one can associate a state by working in a doubled Hilbert space. More explicitly, for an operator \hat{O} , whose matrix representation with respect to the orthonormal basis $\{|m\rangle\}$ is given by

$$\hat{O} = \sum_{m,n} \hat{O}_{m,n} |m\rangle \langle n| \quad \text{where} \quad \hat{O}_{m,n} = \langle m | \hat{O} | n \rangle ,$$

one can associate a state with this operator via [57, 58]

$$\hat{O} = \sum_{m,n} \hat{O}_{m,n} |m\rangle \langle n| \quad \longleftrightarrow \quad |\hat{O}\rangle = \frac{1}{\sqrt{\text{Tr}[\hat{O}^\dagger \hat{O}]}} \sum_{m,n} \hat{O}_{n,m} |m\rangle_{\text{in}} \otimes |n\rangle_{\text{out}} . \quad (4.5)$$

Considering explicitly $\hat{\rho}_A^{1/2}$ and working in the position representation, one has an effective wave function (in this doubled Hilbert space)

$$\psi(x, x') = \frac{1}{\sqrt{\text{Tr}[(\hat{\rho}_A^{1/2})^\dagger \hat{\rho}_A^{1/2}]}} \rho_A^{1/2}(x', x) . \quad (4.6)$$

We will use this as the target state and compute complexity. We can write the wavefunction explicitly as follows:

$$\psi(x'_1, x_1) = \mathcal{N} \exp \left(-\frac{1}{2}(\gamma + \eta)x_1^2 - \frac{1}{2}(\gamma^* + \eta)x_1'^2 + \sqrt{2\eta(\gamma_1 + \eta)}x_1x_1' \right) . \quad (4.7)$$

Here \mathcal{N} is a normalization constant. The effective wave function can be written in the form

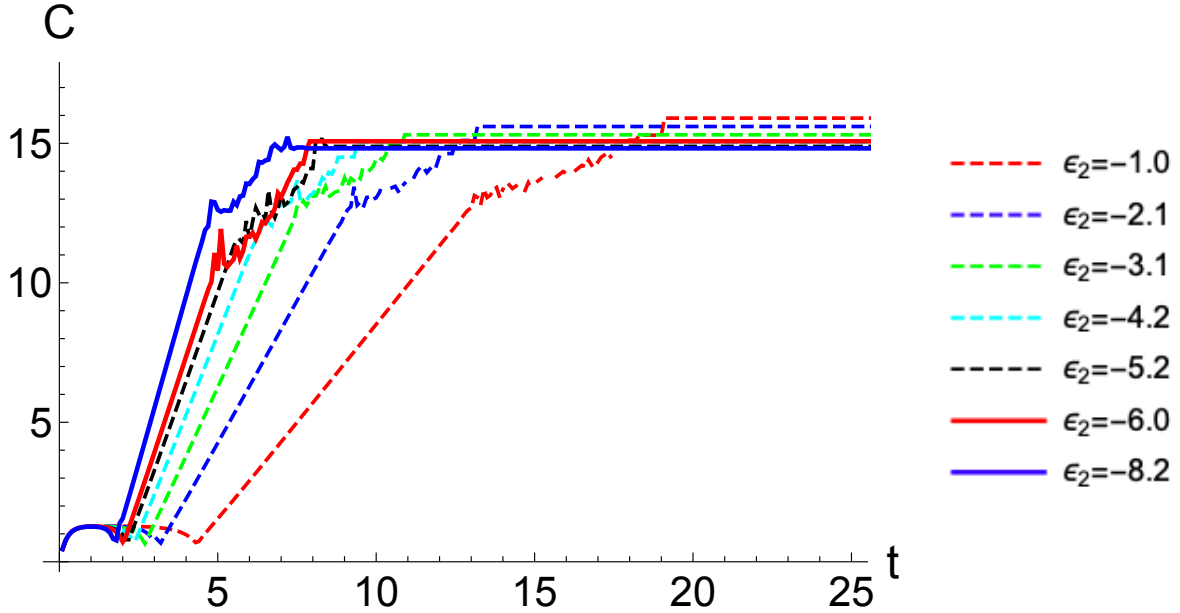


Figure 6: Complexity with fixed $\epsilon_1 = -6, \lambda = 0.1$

$$\psi(x'_1, x_1) = \mathcal{N} \exp \left(-\frac{1}{2} (\beta x_1^2 + \beta^* x_1'^2) + \zeta x_1 x_1' \right) . \quad (4.8)$$

To proceed, we need to diagonalize the argument of the exponential; we obtain the effective wave function

$$\psi(x', x) = \mathcal{N} \exp \left(-\frac{1}{2}(\beta_1 + E)X_1^2 - \frac{1}{2}(\beta_1 - E)X_2^2 \right) \quad (4.9a)$$

where

$$\begin{pmatrix} X_1 \\ X_2 \end{pmatrix} = \begin{pmatrix} u & -v \\ v & u \end{pmatrix} \begin{pmatrix} x_1 \\ x'_1 \end{pmatrix} \quad (4.9b)$$

and

$$E^2 = \zeta^2 - \beta_2^2, \quad u = \sqrt{\frac{1}{2} \left(1 + i \frac{\beta_2}{E} \right)}, \quad v = -\sqrt{\frac{1}{2} \left(1 - i \frac{\beta_2}{E} \right)}, \quad (4.9c)$$

with $\beta_1 = \text{Re}[\beta]$, $\beta_2 = \text{Im}[\beta]$. In what follows, we will use this effective wavefunction (4.9b) as the target state and compute the complexity with respect to the ground state wavefunction.

Fig. 4 represents the complexity for this state (4.9a). When both the system and bath are inverted ($\epsilon_1 < 0, \epsilon_2 < 0$) the complexity for the effective wavefunction displays the expected chaotic like behaviour, namely it contains a small complexity scrambling period, followed by a linear growth and finally a saturation. On top of that, we see a downward concavity during the scrambling region. Note that unlike the full system complexity, when one of the oscillators is inverted, we do not see this behaviour as illustrated in the right panel of Fig. 4. Understanding the physical meaning of this early time behaviour of complexity from the density matrix requires further investigation, and we would leave that for different work.

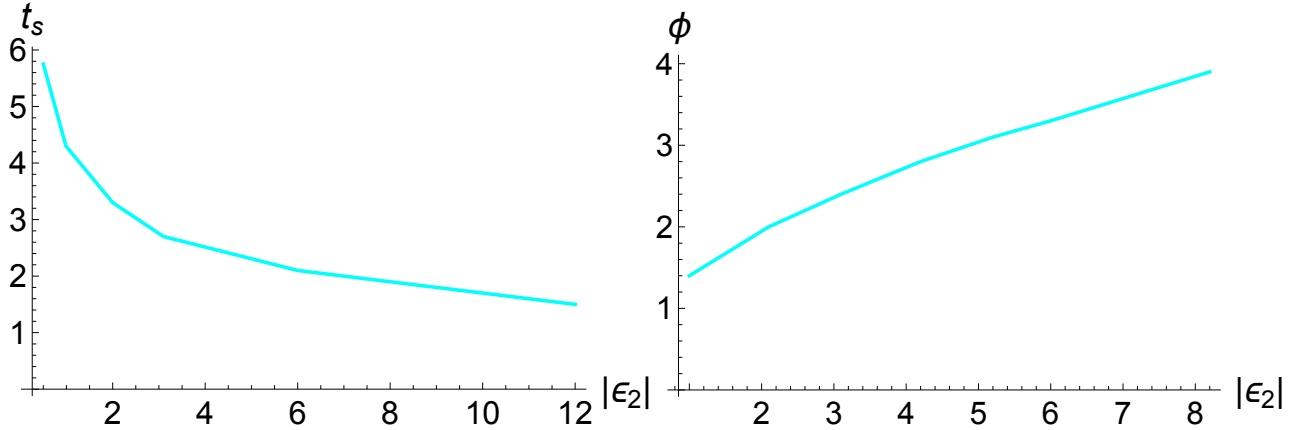


Figure 7: Left: Scrambling time (t_s) vs $|\epsilon_2|$, **Right:** Slope (ϕ) vs $|\epsilon_2|$

Next, we want to investigate if this new diagnostic can sense the entire Lyapunov spectrum, as could the (full) system complexity. This is detailed in Fig. 5. When we fix the bath parameter $\epsilon_2 (< 0)$ and gradually increase the inverted system parameter (starting with a smaller absolute value than the bath parameter), we see the same behaviour as the system complexity. The linear portion is composed of two different slopes, just like the full system complexity. However, we only see one scrambling regime. When the system and the bath

parameters are close, the slopes are aligned; it remains the same, even if the magnitude of the system parameter is larger than the bath parameter. It gives a bound on the growth of complexity (Lyapunov exponent), and this is controlled by the bath parameter. *This feature is not present in the full system case.* On the other hand, we do not see this feature if

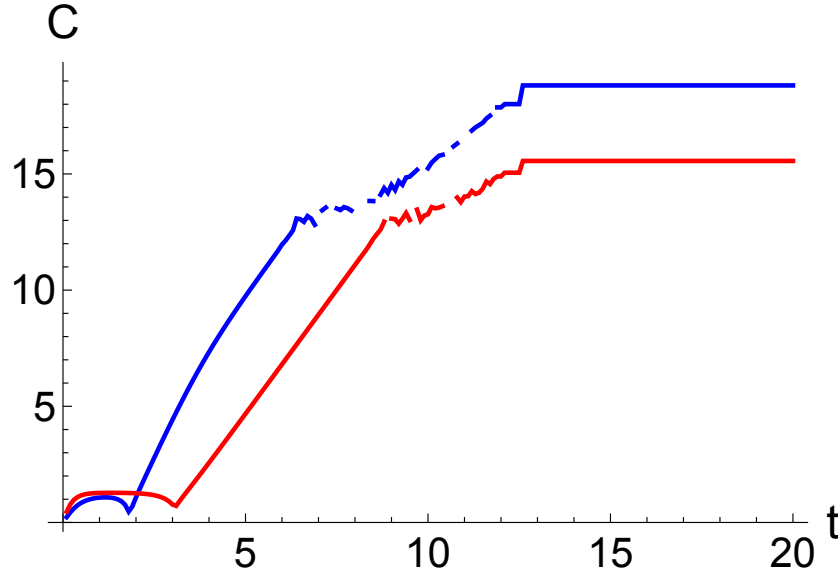


Figure 8: Blue: $\epsilon_1 = -2.3, \epsilon_2 = -6.1, \lambda = 0.1$, Red: $\epsilon_1 = -6.1, \epsilon_2 = -2.3, \lambda = 0.1$

we fix the system parameter $\epsilon_1 (< 0)$ and gradually increase the bath parameter (starting with a smaller absolute value than the system parameter) as in 6. As we change the bath parameter, both the scrambling time and the Lyapunov exponent changes significantly.

We can explore this further by investigating how the scrambling time (time scale when complexity starts to grow linearly [40]) and the slope of the linear growth (Lyapunov exponent) change with changing the bath parameter keeping the system parameter and coupling fixed. The left panel of Fig. 7 displays the change in scrambling time with bath parameter ($|\epsilon_2|$) and the right panel displays the slope with bath parameter ($|\epsilon_2|$). These figures indicate that as the bath gets more unstable/chaotic, the system scrambles faster, and the slope of the complexity grows bigger. Both these behaviours are consistent with the parameter dependence for single oscillator found in [40].

We will conclude this section by highlighting another difference from the full system case. Complexity for this effective wavefunction does not overlap with each other when the parameter ϵ_1 and ϵ_2 are switched as displayed in Fig. 8. The underlying reason for this asymmetry is, of course, the tracing out of the bath oscillator (oscillator 2). This makes it

more appropriate for the understanding of open systems. Since in all realistic scenario, we deal with open systems this complexity provides a more practical choice of investigating the underlying chaotic nature of the system.

4.2 Complexity of Purification

To further illustrate the importance and the scope of our new diagnostic in this section we compute the complexity of purification [17, 28, 60, 61], yet another method of computing complexity for mixed state. We will show that this particular approach is not as sensitive as the operator-state mapping [57–59].

We start with with density (reduced) matrix (4.3a). First we purify ($|\psi_{11'}\rangle$) in such way that,

$$\hat{\rho}_1 = \text{Tr}_{1'} |\psi_{11'}\rangle \langle \psi_{11'}|, \quad (4.10)$$

$1'$ corresponds to the auxiliary Hilbert-space such that $|\psi_{11'}\rangle$ is a pure state. Then the complexity of purification (\mathcal{C}_p) is defined as,

$$\mathcal{C}_p = \min_{1'} \mathcal{C}(|\psi_{11'}\rangle), \quad (4.11)$$

where, the minimization is over all possible purification and $\mathcal{C}(|\psi_{11'}\rangle)$ corresponds to the complexity of the state $|\psi_{11'}\rangle$ with respect to the reference state, which is the ground state of the Hamiltonian (2.1) with $\epsilon_1 = \epsilon_2 = \omega_0 = 1$ and $\lambda = 0$. Also, we choose to use minimal purification as advocated in [28, 71, 72] such that the size of the original (sub) system is same as the auxiliary system. In our case the subsystem is just one oscillator.

Next we parametrize our purified state in the following way,

$$\psi(x_1, x_2) = \mathcal{N} \exp \left(-\frac{1}{2} \left[\alpha x_1^2 + \gamma x_2^2 - 2 \tau x_1 x_2 \right] \right), \quad (4.12)$$

where x_2 belongs to the auxiliary Hilbert-space. α, γ and τ are in general complex and yet to be determined. \mathcal{N} is the normalization of the wavefunction. Then we have

$$\rho(x_1, x_2 | x'_1, x'_2) = \psi(x_1, x_2) \psi^*(x'_1, x'_2) \quad (4.13)$$

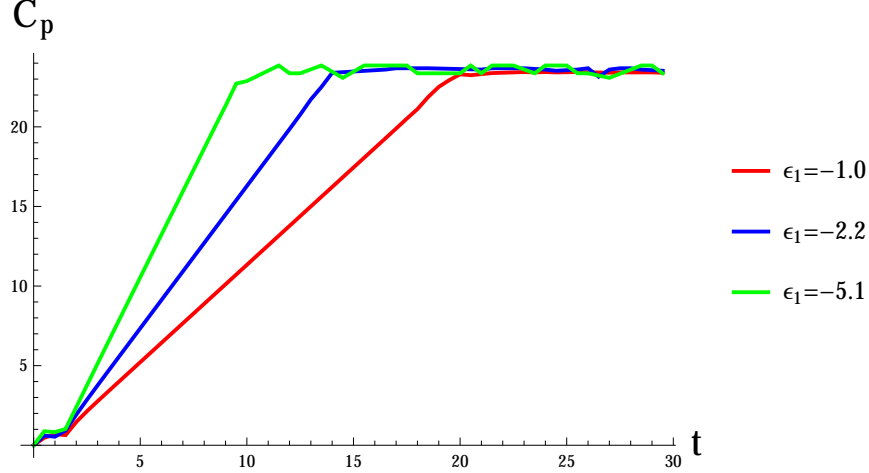


Figure 9: Evolution of Complexity of purification for $\epsilon_2 = -5, \lambda = 0.1$

The corresponding reduced density matrix after tracing out the auxiliary Hilbert space is

$$\begin{aligned} \text{Tr}_2 \rho(x_1, x_2 | x'_1, x'_2) &= \int_{-\infty}^{\infty} dx_2 \psi(x_1, x_2) \psi^*(x'_1, x_2) \\ &= \mathcal{N}^2 \exp \left(-\frac{1}{2} \left[\left(\alpha - \frac{\tau^2}{2 \text{Re}(\gamma)} \right) x_1^2 + \left(\alpha^* - \frac{(\tau^*)^2}{2 \text{Re}(\gamma)} \right) x_1'^2 \right] + \frac{|\tau|^2}{2 \text{Re}(\gamma)} x_1 x_1' \right) \end{aligned} \quad (4.14)$$

Using the condition of (4.10) and using (4.3a) we get the following,

$$\alpha = \Omega_1(t), \tau = \kappa(t), \text{Re}(\gamma) = \text{Re}(\Omega_2(t)). \quad (4.15)$$

We have determined all the parameters inside (4.12) in terms of the given parameters as in (4.15), except for $\text{Im}(\gamma)$. Hence the minimization in (4.11) can be carried over $\text{Im}(\gamma)$ and the minimum value will correspond to the complexity of purification. We compute the complexity corresponding to (4.12) as follows:

$$\mathcal{C}(|\psi_{11'}\rangle) = \frac{1}{2} \sqrt{\sum_{i=1}^2 \left[\ln \left(\frac{|\omega_i|}{\omega_0} \right)^2 + \tan^{-1} \left(-\frac{\text{Im}(\omega_i)}{\text{Re}(\omega_i)} \right)^2 \right]}, \quad (4.16)$$

where,

$$\omega_1 = \frac{1}{2}(\alpha + \gamma + \sqrt{(\alpha - \gamma)^2 + 4\tau^2}), \quad \omega_2 = \frac{1}{2}(\alpha + \gamma - \sqrt{(\alpha - \gamma)^2 + 4\tau^2}), \quad \omega_0 = 1. \quad (4.17)$$

Finally, the complexity of purification is

$$\mathcal{C}_p = \min_{\text{Im}(\gamma)} \left(\frac{1}{2} \sqrt{\sum_{i=1}^2 \left[\ln \left(\frac{|\omega_i|}{\omega_0} \right)^2 + \tan^{-1} \left(-\frac{\text{Im}(\omega_i)}{\text{Re}(\omega_i)} \right)^2 \right]} \right). \quad (4.18)$$

In Fig. 9 we display the evolution of this complexity for $\epsilon_2 = -5$, $\lambda = 0.1$ (as we did with the operator-state mapping [57–59]). By comparing with Fig. (5), we can see easily that \mathcal{C}_p gives us a similar early time behaviour. This early time behaviour is then followed by a linear growth as expected for this kind of systems. However, unlike the previous case, we only get a single slope, hence \mathcal{C}_p doesn't give us the information about the Lyapunov spectrum. We can only extract one of the Lyapunov exponents. This complexity is not as sensitive as the complexity of state obtained using operator-state mapping in capturing chaotic behaviour.

5 Discussion

In this work, we took the first step toward using complexity to characterize chaos in a multiparticle system; concomitantly, we took strides in using complexity to characterize open quantum systems. Our model consisted of two oscillators, where one or both of the oscillators is inverted. Since the inverted oscillator is known to capture features similar to chaotic systems [47], this provides a natural toy model to study chaos. By exploring different types of quantum circuits, we showed that complexity is a useful diagnostic of chaos.

We first considered the complexity of a doubly-evolved target state (forward followed by a backward evolutions with slightly different Hamiltonians) $|\psi_T\rangle = \exp(iH_{>}^B t) \exp(-iH_{>}^F t) |\psi_0\rangle$, comparing the results with a singly-evolved target state $|\psi_T\rangle = \exp(-iH_{>} t) |\psi_0\rangle$. We showed that, for both the singly-evolved and doubly-evolved target states, the (full) system complexity exhibited different early-time behaviour, but are both bounded by the same saturation value. When the parameters of the two oscillators are different, the linear growth region of the doubly-evolved state splits into two separate regions. Furthermore, the growth of complexity does not change when the parameters of the two oscillators are switched.

Next, we proposed a more natural diagnostic of chaos-based on the reduced density matrix (where one of the particles is traced out) and the operator-state mapping [57–59]. We discovered that the scrambling time and Lyapunov exponents are mainly dictated by

the parameter of the particle that was traced out, i.e. by the ‘bath’. *This is consistent with the black hole case where the Lyapunov exponent is bounded by the bath temperature* [6]. We compared our results with those obtained using the complexity of purification; we showed that the complexity of purification gives less information, thus further highlighting the importance of the specific construction of our new proposal.

Besides its potential as a more natural testing device for chaotic behaviour, complexity from the density matrix has another advantage over the full system complexity. Indeed, this proposal provides a more *natural* form of complexity to compare with other information-theoretic measures such as Renyi entropy, entanglement entropy, etc., as they all are based on the same quantity, namely the reduced density matrix. Hence, this might open up possibilities to explore complexity as an extension of entropy [73, 74] and other measures of correlations (for eg. OTOC) [75–77] for open systems.

To give a proof-of-principle argument for complexity from the reduced density matrix as a new diagnostic for chaos, we have used the coupled inverted oscillators as a toy model. This is, however, a rather special example and, by no means, a realistic chaotic system. We want to explore this diagnostic for the realistic chaotic system in future work.

Acknowledgements

We would like to thank Jeff Murugan, Bret Underwood, Kaushik Ghosh, Aranya Bhattacharya for helpful conversations and discussions. A.B. is supported by Start Up Research Grant (SRG/2020/001380) by Department of Science & Technology Science and Engineering Research Board (India). S.H. would like to thank the University of Cape Town for funding this project.

References

- [1] Nicholas R Hunter-Jones. “Chaos and Randomness in Strongly-Interacting Quantum Systems.” *Dissertation (Ph.D.), California Institute of Technology*. (2018).
- [2] Viktor Jahnke. “Recent developments in the holographic description of quantum chaos”. *Adv. High Energy Phys.* 2019 (2019), 9632708. arXiv: 1811.06949 [hep-th].

- [3] O. Bohigas, M.J. Giannoni, and C. Schmit. “Characterization of chaotic quantum spectra and universality of level fluctuation laws”. *Phys. Rev. Lett.* 52 (1984), 1–4.
- [4] A. Kitaev. “A simple model of quantum holography”. *Proceedings of the KITP Program: Entanglement in Strongly-Correlated Quantum Matter*, (Kavli Institute for Theoretical Physics, Santa Barbara) Vol. 7 (2015).
- [5] A. I. Larkin and Yu. N. Ovchinnikov. “Quasiclassical Method in the Theory of Superconductivity”. *Soviet Journal of Experimental and Theoretical Physics* 28 (June 1969), 1200.
- [6] Juan Maldacena, Stephen H. Shenker, and Douglas Stanford. “A bound on chaos”. *Journal of High Energy Physics* 2016.8 (Aug. 2016). ISSN: 1029-8479.
- [7] Koji Hashimoto, Keiju Murata, and Ryosuke Yoshii. “Out-of-time-order correlators in quantum mechanics”. *JHEP* 10 (2017), 138. arXiv: 1703.09435 [hep-th].
- [8] M. A. Nielsen. “A geometric approach to quantum circuit lower bounds”. *Science* 311.4 (2006), 92. arXiv: 0502070 [quant-ph].
- [9] M. R. Nielsen M. A. and Dowling, M. Gu, and A. M. Doherty. “Quantum Computation as Geometry”. *Science* 311.4 (2006), 1133–1135. arXiv: 0603161 [quant-ph].
- [10] M. R. Nielsen M. A. and Dowling. “The geometry of quantum computation”. *Science* 311.4 (2006), 1133–1135. arXiv: 0701004 [quant-ph].
- [11] Ro Jefferson and Robert C. Myers. “Circuit complexity in quantum field theory”. *JHEP* 10 (2017), 107. arXiv: 1707.08570 [hep-th].
- [12] Shira Chapman, Michal P. Heller, Hugo Marrochio, and Fernando Pastawski. “Toward a Definition of Complexity for Quantum Field Theory States”. *Phys. Rev. Lett.* 120.12 (2018), 121602. arXiv: 1707.08582 [hep-th].
- [13] Pawel Caputa, Nilay Kundu, Masamichi Miyaji, Tadashi Takayanagi, and Kento Watanabe. “Liouville Action as Path-Integral Complexity: From Continuous Tensor Networks to AdS/CFT”. *JHEP* 11 (2017), 097. arXiv: 1706.07056 [hep-th].
- [14] Arpan Bhattacharyya, Arvind Shekar, and Aninda Sinha. “Circuit complexity in interacting QFTs and RG flows”. *JHEP* 10 (2018), 140. arXiv: 1808.03105 [hep-th].
- [15] Lucas Hackl and Robert C. Myers. “Circuit complexity for free fermions”. *JHEP* 07 (2018), 139. arXiv: 1803.10638 [hep-th].

- [16] Rifath Khan, Chethan Krishnan, and Sanchita Sharma. “Circuit Complexity in Fermionic Field Theory”. *Phys. Rev. D* 98.12 (2018), 126001. arXiv: 1801.07620 [hep-th].
- [17] Hugo A. Camargo, Pawel Caputa, Diptarka Das, Michal P. Heller, and Ro Jefferson. “Complexity as a novel probe of quantum quenches: universal scalings and purifications”. *Phys. Rev. Lett.* 122.8 (2019), 081601. arXiv: 1807.07075 [hep-th].
- [18] Tibra Ali, Arpan Bhattacharyya, S. Shajidul Haque, Eugene H. Kim, and Nathan Moynihan. “Post-Quench Evolution of Complexity and Entanglement in a Topological System” (2018). arXiv: 1811.05985 [hep-th].
- [19] Arpan Bhattacharyya, Pawel Caputa, Sumit R. Das, Nilay Kundu, Masamichi Miyaji, and Tadashi Takayanagi. “Path-Integral Complexity for Perturbed CFTs”. *JHEP* 07 (2018), 086. arXiv: 1804.01999 [hep-th].
- [20] Pawel Caputa and Javier M. Magan. “Quantum Computation as Gravity”. *Phys. Rev. Lett.* 122.23 (2019), 231302. arXiv: 1807.04422 [hep-th].
- [21] Arpan Bhattacharyya, Pratik Nandy, and Aninda Sinha. “Renormalized Circuit Complexity”. *Phys. Rev. Lett.* 124.10 (2020), 101602. arXiv: 1907.08223 [hep-th].
- [22] Pawel Caputa and Ian MacCormack. “Geometry and Complexity of Path Integrals in Inhomogeneous CFTs” (Apr. 2020). arXiv: 2004.04698 [hep-th].
- [23] Mario Flory and Michal P. Heller. “Complexity and Conformal Field Theory” (May 2020). arXiv: 2005.02415 [hep-th].
- [24] Johanna Erdmenger, Marius Gerbershagen, and Anna-Lena Weigel. “Complexity measures from geometric actions on Virasoro and Kac-Moody orbits” (Apr. 2020). arXiv: 2004.03619 [hep-th].
- [25] Arpan Bhattacharyya, Saurya Das, S. Shajidul Haque, and Bret Underwood. “Cosmological complexity”. *Physical Review D* 101.10 (May 2020). ISSN: 2470-0029.
- [26] Arpan Bhattacharyya, Saurya Das, S. Shajidul Haque, and Bret Underwood. “Rise of cosmological complexity: Saturation of growth and chaos”. *Physical Review Research* 2.3 (Aug. 2020). ISSN: 2643-1564.
- [27] Giuseppe Di Giulio and Erik Tonni. “Complexity of mixed Gaussian states from Fisher information geometry” (June 2020). arXiv: 2006.00921 [hep-th].
- [28] Elena Caceres, Shira Chapman, Josiah D. Couch, Juan P. Hernandez, Robert C. Myers, and Shan-Ming Ruan. “Complexity of Mixed States in QFT and Holography”. *JHEP* 03 (2020), 012. arXiv: 1909.10557 [hep-th].

- [29] Leonard Susskind and Ying Zhao. “Complexity and Momentum” (June 2020). arXiv: 2006.03019 [hep-th].
- [30] Bowen Chen, Bartłomiej Czech, and Zi-zhi Wang. “Cutoff Dependence and Complexity of the CFT₂ Ground State” (Apr. 2020). arXiv: 2004.11377 [hep-th].
- [31] Bartłomiej Czech. “Einstein Equations from Varying Complexity”. *Phys. Rev. Lett.* 120.3 (2018), 031601. arXiv: 1706.00965 [hep-th].
- [32] Hugo A. Camargo, Michal P. Heller, Ro Jefferson, and Johannes Knaute. “Path integral optimization as circuit complexity”. *Phys. Rev. Lett.* 123.1 (2019), 011601. arXiv: 1904.02713 [hep-th].
- [33] Shira Chapman, Jens Eisert, Lucas Hackl, Michal P. Heller, Ro Jefferson, Hugo Marrochio, and Robert C. Myers. “Complexity and entanglement for thermofield double states”. *SciPost Phys.* 6.3 (2019), 034. arXiv: 1810.05151 [hep-th].
- [34] Shira Chapman and Hong Zhe Chen. “Complexity for Charged Thermofield Double States” (Oct. 2019). arXiv: 1910.07508 [hep-th].
- [35] Mehregan Doroudiani, Ali Naseh, and Reza Pirmoradian. “Complexity for Charged Thermofield Double States”. *JHEP* 01 (2020), 120. arXiv: 1910.08806 [hep-th].
- [36] Hao Geng. “ $T\bar{T}$ Deformation and the Complexity=Volume Conjecture”. *Fortsch. Phys.* 68.7 (2020), 2000036. arXiv: 1910.08082 [hep-th].
- [37] Minyong Guo, Zhong-Ying Fan, Jie Jiang, Xiangjing Liu, and Bin Chen. “Circuit complexity for generalized coherent states in thermal field dynamics”. *Phys. Rev. D* 101.12 (2020), 126007. arXiv: 2004.00344 [hep-th].
- [38] Leonard Susskind. “Computational Complexity and Black Hole Horizons”. *Fortsch. Phys.* 64 (2016). [Addendum: *Fortsch. Phys.* 64, 44–48 (2016)], 24–43. arXiv: 1403.5695 [hep-th].
- [39] Leonard Susskind. “Entanglement is not enough”. *Fortsch. Phys.* 64 (2016), 49–71. arXiv: 1411.0690 [hep-th].
- [40] Tibra Ali, Arpan Bhattacharyya, S. Shajidul Haque, Eugene H. Kim, Nathan Moynihan, and Jeff Murugan. “Chaos and Complexity in Quantum Mechanics”. *Phys. Rev. D* 101.2 (2020), 026021. arXiv: 1905.13534 [hep-th].
- [41] A. Bhattacharyya, W. Chemissany, S. Shajidul Haque, and B. Yan. “Towards the Web of Quantum Chaos Diagnostics” (Sept. 2019). arXiv: 1909.01894 [hep-th].

- [42] Jonah Kudler-Flam, Laimei Nie, and Shinsei Ryu. “Conformal field theory and the web of quantum chaos diagnostics”. *JHEP* 01 (2020), 175. arXiv: 1910.14575 [hep-th].
- [43] Arpan Bhattacharyya, Wissam Chemissany, S. Shajidul Haque, Jeff Murugan, and Bin Yan. “The Multi-faceted Inverted Harmonic Oscillator: Chaos and Complexity” (2020). arXiv: 2007.01232 [hep-th].
- [44] Vijay Balasubramanian, Matthew Decross, Arjun Kar, and Onkar Parrikar. “Quantum Complexity of Time Evolution with Chaotic Hamiltonians”. *JHEP* 01 (2020), 134. arXiv: 1905.05765 [hep-th].
- [45] Run-Qiu Yang and Keun-Young Kim. “Time evolution of the complexity in chaotic systems: a concrete example”. *JHEP* 05 (2020), 045. arXiv: 1906.02052 [hep-th].
- [46] Run-Qiu Yang, Yu-Sen An, Chao Niu, Cheng-Yong Zhang, and Keun-Young Kim. “To be unitary-invariant or not?: a simple but non-trivial proposal for the complexity between states in quantum mechanics/field theory” (June 2019). arXiv: 1906.02063 [hep-th].
- [47] R. Blume-Kohout and W. H. Zurek. “Decoherence from a chaotic environment: An upside-down “oscillator” as a model”. *Physical Review A* 68.3 (Sept. 2003), 032104. ISSN: 1050-2947.
- [48] T. Morita. “Thermal Emission from Semiclassical Dynamical Systems”. *Physical Review Letters* 122.10 (Mar. 2019), 101603. ISSN: 0031-9007, 1079-7114.
- [49] P. Bueno, J. M Magan, and C. S. Shahbazi. “Complexity measures in QFT and constrained geometric actions” (Aug. 2019). arXiv: 1908.03577 [hep-th].
- [50] Bin Yan, Lukasz Cincio, and Wojciech H Zurek. “Information Scrambling and Loschmidt Echo”. *Physical Review Letters* 124.16 (Apr. 2020), 160603. ISSN: 0031-9007.
- [51] Panagiotis Betzios, Nava Gaddam, and Olga Papadoulaki. “The Black Hole S-Matrix from Quantum Mechanics”. *JHEP* 11 (2016), 131. arXiv: 1607.07885 [hep-th].
- [52] Panos Betzios, Nava Gaddam, and Olga Papadoulaki. “Black holes, quantum chaos, and the Riemann hypothesis” (Apr. 2020). arXiv: 2004.09523 [hep-th].
- [53] Suraj S. Hegde, Varsha Subramanyan, Barry Bradlyn, and Smitha Vishveshwara. “Quasinormal Modes and the Hawking-Unruh Effect in Quantum Hall Systems: Lessons from Black Hole Phenomena”. *Phys. Rev. Lett.* 123.15 (2019), 156802. arXiv: 1812.08803 [cond-mat.mes-hall].

- [54] Koji Hashimoto, Kyoung-Bum Huh, Keun-Young Kim, and Ryota Watanabe. “Exponential growth of out-of-time-order correlator without chaos: inverted harmonic oscillator” (July 2020). arXiv: 2007.04746 [hep-th].
- [55] S. Shajidul Haque and Bret Underwood. “The Squeezed OTOC and Cosmology” (2020). arXiv: 2010.08629 [hep-th].
- [56] Hrant Gharibyan, Masanori Hanada, Brian Swingle, and Masaki Tezuka. “Quantum Lyapunov Spectrum”. *JHEP* 04 (2019), 082. arXiv: 1809.01671 [quant-ph].
- [57] A. Jamiolkowski. “Linear transformations which preserve trace and positive semidefiniteness of operators”. *Reports on Mathematical Physics* 3.4 (1972), 275–278. ISSN: 0034-4877.
- [58] Man-Duen Choi. “Completely positive linear maps on complex matrices”. *Linear Algebra and its Applications* 10.3 (1975), 285–290. ISSN: 0024-3795.
- [59] Min Jiang, Shunlong Luo, and Shuangshuang Fu. “Channel-state duality”. *Phys. Rev. A* 87 (2 Feb. 2013), 022310.
- [60] Cesar A. Agon, Matthew Headrick, and Brian Swingle. “Subsystem complexity and holography”. *Journal of High Energy Physics* 2019.2 (Feb. 2019). ISSN: 1029-8479.
- [61] Hugo A. Camargo, Lucas Hackl, Michal P. Heller, Alexander Jahn, Tadashi Takayanagi, and Bennet Windt. “Entanglement and Complexity of Purification in (1+1)-dimensional free Conformal Field Theories” (Sept. 2020). arXiv: 2009.11881 [hep-th].
- [62] Aranya Bhattacharya, Kevin T. Grosvenor, and Shibaji Roy. “Entanglement Entropy and Subregion Complexity in Thermal Perturbations around Pure-AdS Spacetime”. *Phys. Rev. D* 100.12 (2019), 126004. arXiv: 1905.02220 [hep-th].
- [63] Bin Chen, Wen-Ming Li, Run-Qiu Yang, Cheng-Yong Zhang, and Shao-Jun Zhang. “Holographic subregion complexity under a thermal quench”. *JHEP* 07 (2018), 034. arXiv: 1803.06680 [hep-th].
- [64] A. O. Caldeira and A. J. Leggett. “Influence of Dissipation on Quantum Tunneling in Macroscopic Systems”. *Phys. Rev. Lett.* 46 (4 Jan. 1981), 211–214.
- [65] A.O Caldeira and A.J Leggett. “Quantum tunnelling in a dissipative system”. *Annals of Physics* 149.2 (1983), 374–456. ISSN: 0003-4916.
- [66] I. Rotter and J. P. Bird. “A review of progress in the physics of open quantum systems: theory and experiment”. *Reports on Progress in Physics* 78.11, 114001 (Nov. 2015), 114001. arXiv: 1507.08478 [quant-ph].

- [67] Tibra Ali, Arpan Bhattacharyya, S. Shajidul Haque, Eugene H. Kim, and Nathan Moynihan. “Time Evolution of Complexity: A Critique of Three Methods”. *JHEP* 04 (2019), 087. arXiv: 1810.02734 [hep-th].
- [68] Thomas Gorin, Tomaž Prosen, Thomas H. Seligman, and Marko Žnidarič. “Dynamics of Loschmidt echoes and fidelity decay”. *Physics Reports* 435.2-5 (Nov. 2006), 33–156. ISSN: 0370-1573.
- [69] Arseni Goussev, Rodolfo A. Jalabert, Horacio M. Pastawski, and Diego Wisniacki. “Loschmidt Echo”. *arXiv e-prints*, arXiv:1206.6348 (June 2012), arXiv:1206.6348. arXiv: 1206.6348 [nlin.CD].
- [70] Amin A. Nizami. “Quantum chaos measures for Floquet dynamics” (July 2020). arXiv: 2007.07283 [quant-ph].
- [71] Arpan Bhattacharyya, Tadashi Takayanagi, and Koji Umemoto. “Entanglement of Purification in Free Scalar Field Theories”. *JHEP* 04 (2018), 132. arXiv: 1802.09545 [hep-th].
- [72] Arpan Bhattacharyya, Alexander Jahn, Tadashi Takayanagi, and Koji Umemoto. “Entanglement of Purification in Many Body Systems and Symmetry Breaking”. *Phys. Rev. Lett.* 122.20 (2019), 201601. arXiv: 1902.02369 [hep-th].
- [73] Adam R. Brown and Leonard Susskind. “Second law of quantum complexity”. *Phys. Rev. D* 97.8 (2018), 086015. arXiv: 1701.01107 [hep-th].
- [74] Alice Bernamonti, Federico Galli, Juan Hernandez, Robert C. Myers, Shan-Ming Ruan, and Joan Simón. “First Law of Holographic Complexity”. *Phys. Rev. Lett.* 123.8 (2019), 081601. arXiv: 1903.04511 [hep-th].
- [75] S.V. Syzranov, A.V. Gorshkov, and V. Galitski. “Out-of-time-order correlators in finite open systems”. *Phys. Rev. B* 97.16 (2018), 161114. arXiv: 1704.08442 [cond-mat.mes-hall].
- [76] Jan Tuziemski. “Out-of-time-ordered correlation functions in open systems: A Feynman-Vernon influence functional approach”. *Phys. Rev. A* 100.6 (2019), 062106. arXiv: 1903.05025 [quant-ph].
- [77] Bidisha Chakrabarty, Soumyadeep Chaudhuri, and R. Loganayagam. “Out of Time Ordered Quantum Dissipation”. *JHEP* 07 (2019), 102. arXiv: 1811.01513 [cond-mat.stat-mech].